Relationship between Electron Spin Polarization, Electron Exchange Interaction, and Lifetime: The Excited Multiplet States of Phthalocyaninatosilicon Covalently Linked to One Nitroxide Radical

Kazuyuki Ishii, Shoji Takeuchi, and Nagao Kobayashi*

Department of Chemistry, Graduate School of Science, Tohoku University, Sendai 980-8578, Japan

Received: December 31, 2000; In Final Form: March 26, 2001

We have studied phthalocyaninatosilicon (SiPc) covalently linked to one nitroxide radical by the combined use of transient absorption and time-resolved electron paramagnetic resonance (TREPR) spectroscopies and succeeded in clarifying the relationship between the electron spin polarization (ESP), excited-state lifetime, and electron exchange interaction between the excited triplet SiPc and doublet nitroxide. It is found that the lifetime of the excited triplet SiPc is dependent on the linking nitroxide radical and correlates well with the magnitude of the electron exchange interaction. The ESPs due to both D_1-Q_1 mixing (the D_1 and Q_1 states consist of the excited triplet SiPc and doublet nitroxide radical) and spin−orbit coupling (SOC) are observed by systematically changing the electron exchange interaction. It is found that the ESP of the radical−triplet pair changes from SOC type to D_1-Q_1 mixing type with increasing degree of electron exchange interaction. These relationships are important for understanding the excited-state dynamics of the radical−triplet pair system.

Introduction

Interactions between photoexcited triplet molecules and paramagnetic species result in some important phenomena, such as quenching of photoexcited molecules[1,2] and generation of the excited singlet oxygen.[3] A time-resolved electron paramagnetic resonance (TREPR) method, which is a powerful technique for observing paramagnetic intermediates after photoexcitation, has been shown to be useful for investigating the interactions between photoexcited triplet molecules and other paramagnetic molecules.[4−9] Recently, some chromophores bonded to paramagnetic molecules have been studied in order to achieve a direct investigation of excited multiplet states consisting of a photoexcited triplet chromophore and doublet molecules.[6−9] The lowest excited doublet (D_1) and quartet (Q_1) states, which consist of the excited triplet chromophore and doublet nitroxide (NO) radical, have been observed in solution for several systems, where the electron spin polarizations (ESPs) in the Q_1 state are divided into two groups. The first group contains fullerene covalently linked to a nitroxide radical (C_{60}−NO), and metalloporphyrin coordinated by a pyridyl nitronyl nitroxide radical (MP−nitpy).[6,7] In these systems, the ESP is reversed with time and has been interpreted by the D_1-Q_1 mixing. The other group is tetra-*tert*-butylphthalocyaninatosilicon (SiPc) covalently linked to one NO radical (R1c, Chart 1).[8a] In this system, the ESP in the Q_1 state decays without ESP inversion, which has been explained by spin−orbit coupling (SOC) between the excited doublet and Q_1 states. While these ESPs are important for understanding the excited-state dynamics, a relationship between the two types of ESP behavior has not been examined experimentally and needs to be clarified.

In this report, we have studied some SiPcs covalently linked to one NO radical (Chart 1) by the combined use of transient absorption and TREPR techniques. Since it has been shown for metal−nitroxide interactions that the electron exchange interaction of the PROXYL (2,2,5,5-tetramethyl-1-pyrrolidinyloxy) derivative is about 15 times that of the TEMPO (2,2,6,6-tetramethyl-1-piperidinyloxy) derivative,[10] the electron exchange interaction in our system can be changed as required. Furthermore, a comparison between R1a (R1c) and R1b (R1d) is suitable for investigating the role of the −O− and −OCO− bridges. In this paper, the relationship between the ESP in the Q_1 state, excited-state lifetime, and electron exchange interaction is discussed and clarified.

CHART 1

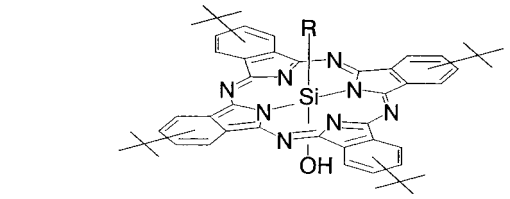

Compound	R0	R1a	R1b	R1c	R1d
R—	HO—				

Experimental Section

Materials. R0 and R1c were synthesized following the methods previously reported.[8] 3-Carboxy-PROXYL and 4-carboxy-TEMPO were purchased from Tokyo Chemical Industry Co, Ltd. and Aldrich Chemical Co., respectively. 3-Hydroxy-PROXYL was prepared from 3-carbamido-2,2,5,5-tetramethyl-

* To whom correspondence should be addressed.

10.1021/jp010077p CCC: $20.00
Published on Web 06/20/2001

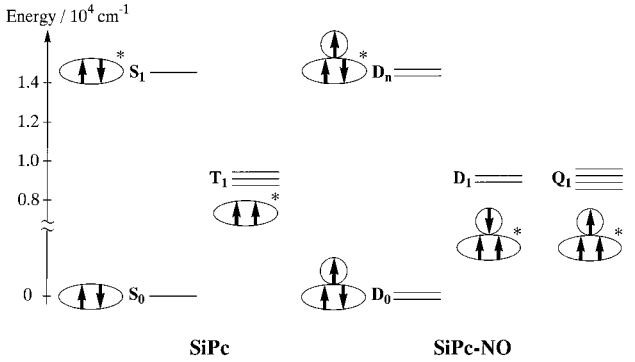

Figure 1. Energy diagrams of SiPc and SiPc−NO.

1-pyrrolidinyloxy with reference to the method previously reported.[11] R1a, R1b, and R1d were synthesized in analogy with R1c.[6] For R1a, R0 and 3-hydroxy-PROXYL were refluxed in toluene for 1 day. For R1b and R1d, 3-carboxy-PROXYL and 4-carboxy-TEMPO, respectively, were refluxed with R0 in pyridine for 1 day. After neutral alumina and gel permeation (Bio-Beads SX-1 or SX-8, Bio-Rad) chromatography, R1a, R1b, and R1d were isolated in 37%, 15%, and 9% yields, respectively. UV−vis, FAB-mass, and elemental analyses were satisfactory, as follows.

R1a: UV−vis (λ/nm (ϵ/10^4)) 680.5 (28.0), 651.0 (3.76), 612.0 (4.41), 360.0 (8.90); FAB mass *m*/*e* 938 (M^+). Anal. Calcd for $C_{56}H_{64}N_9O_3Si$: C, 71.61; H, 6.87; N, 13.42. Found: C, 70.893; H, 6.633; N, 12.766.

R1b: UV−vis (λ/nm (ϵ/10^4)) 685.0 (23.6), 653.0 (3.61), 616.5 (3.77), 362.0 (7.75); FAB mass *m*/*e* 966 (M^+). Anal. Calcd for $C_{57}H_{64}N_9O_4Si$: C, 70.78; H, 6.67; N, 13.03. Found: C, 70.622; H, 6.503; N, 12.251.

R1d: UV−vis (λ/nm (ϵ/10^4)) 685.5 (24.2), 656.0 (3.33), 616.5 (3.72), 362.5 (7.64); FAB mass *m*/*e* 980 (M^+). Anal. Calcd for $C_{58}H_{66}N_9O_4Si$: C, 70.99; H, 6.78; N, 12.85. Found: C, 71.997; H, 7.133; N, 11.955.

Measurements. Spectral-grade toluene (Nacalai Tesque Inc.) was used as a solvent for all measurements. Compounds were purified carefully before the measurements. The concentrations of samples were 1×10^{-4} and 1×10^{-3} M for transient absorption and TREPR measurements, respectively. Samples were deaerated by freeze−pump−thaw cycles, and then the measurements were carried out within 2 days.

Transient absorption measurements were performed at room temperature by using a monochromator (JASCO CT-25CP) and a photomultiplier (Hamamatsu Photonics R446) with a continuous wave of metal halide lamp (Sigma Koki IMH-250).[8d] TREPR, pulse-EPR, and steady-state EPR measurements were carried out on a Bruker ESP 300E spectrometer.[7,8,12] An Oxford ESR 900 cold gas flow system was used for controlling temperature. For the transient absorption and TREPR measurements, samples were excited at 620 or 585 nm by a dye laser (Lumonics HD 500) pumped with a excimer laser (Lumonics EX 500, 13 ns fwhm), and the signals were integrated using a digital oscilloscope (Iwatsu-LeCroy LT342 or LeCroy 9450A).

Theoretical Background

Simple energy diagrams of the excited states of SiPc and SiPc-NO are shown in Figure 1. For SiPc, the lowest excited singlet (S_1) state is almost derived from the $^1(a_{1u}e_g)$ configuration [the $a_{1u}(\pi)$ and $e_g(\pi^*)$ orbitals denote the HOMO and LUMO of Pc ligand, respectively] and is located at ~14 500 cm^{-1}. The lowest excited triplet (T_1) state also originates from the $^3(a_{1u}e_g)$ configuration and is located at ~9000 cm^{-1}.[13]

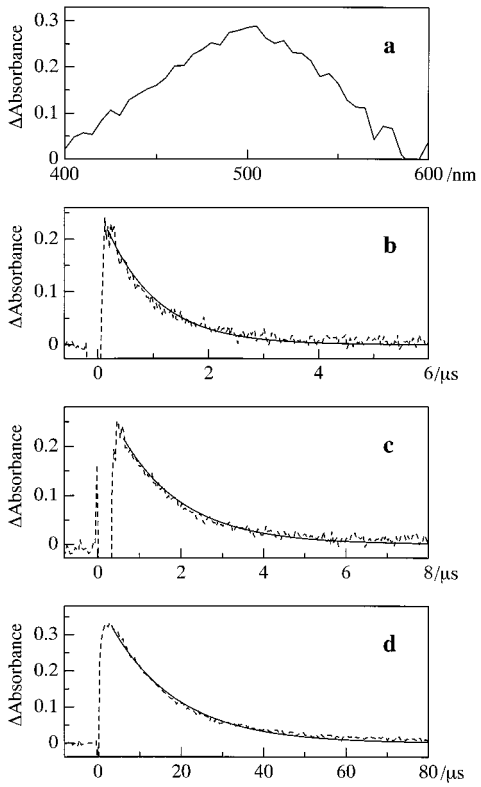

Figure 2. Transient absorption spectrum of R1d (a) and decay profiles of transient absorption signals (broken lines) of R1a (b), R1b (c), and R1d (d) at 490 nm, together with fitted curves (solid lines). The transient absorption spectrum was observed at 6.5 μs after 620 nm laser excitation. Fitted curves were calculated by a least-squares method.

TABLE 1: Lifetimes of the Excited Triplet SiPc Measured by Transient Absorption Signals

compound	R1a	R1b	R1c	R1d	R0
lifetime/μs	0.86 ± 0.08	1.4 ± 0.12	7.6 ± 0.3	15 ± 0.9	500 ± 30

For SiPc-NO, the doublet ground (D_0) state consists of NO in the D_0 state and SiPc in the singlet ground (S_0) state. A pair of the D_0 NO and S_1 SiPc provides the excited doublet (D_n) state. On the other hand, the lowest excited doublet (D_1) and quartet (Q_1) states are generated by an interaction between the D_0 NO and T_1 SiPc.

Results and Interpretations

Transient Absorption Measurements. Transient absorption measurements were carried out for R1a, R1b, and R1d. A typical transient absorption spectrum of R1d is shown in Figure 2a. Transient absorption spectra of all complexes are almost identical to that of R0,[2b,14] indicating that the electronic interaction between the excited triplet SiPc and doublet NO is weak.[8d] Decay profiles of the transient absorption signals are shown in Figure 2 and were analyzed with single-exponential functions.[15] The lifetimes of R1a, R1b, and R1d were evaluated as 0.86, 1.4, and 15 μs (Table 1), respectively, which are much shorter than that (=500 μs) of R0.[8d]

In comparison with the lifetime (=7.6 μs) of R1c, it is found that the lifetime of the excited triplet SiPc is markedly dependent on the linking NO radical. It is noteworthy that the lifetimes of R1a (=0.86 μs) and R1b (=1.4 μs) are about $^1/_{10}$ of those of R1c (=7.6 μs) and R1d (=15 μs), respectively. These relationships can be reasonably interpreted by considering that the PROXYL derivatives have the stronger electron exchange interaction than the TEMPO derivatives because of the shorter

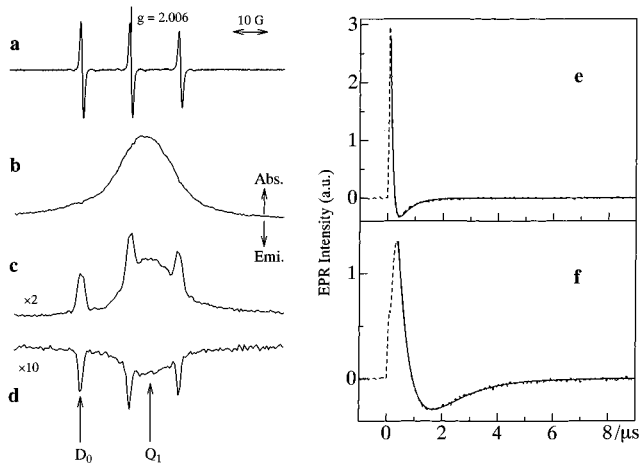

Figure 3. Steady-state EPR spectrum (a), TREPR spectra (b, c, d), and time profiles of the Q_1 and D_0 signals (e, f; broken lines) of R1a, together with fitted curves (e, f; solid lines). TREPR spectra were observed at 0.1 (b), 0.2 (c), and 1.6 (d) μs after 585 nm laser excitation. Time profiles of the Q_1 and D_0 signals were measured at positions indicated by the Q_1 and D_0 arrows, respectively. Fitted curves were calculated by a least-squares method.

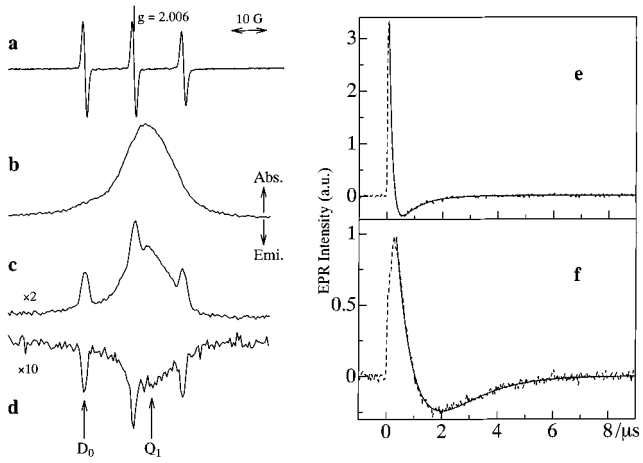

Figure 4. Steady-state EPR spectrum (a), TREPR spectra (b, c, d), and time profiles of the Q_1 and D_0 signals (e, f; broken lines) of R1b, together with fitted curves (e, f; solid lines). TREPR spectra were observed at 0.1 (b), 0.2 (c), and 1.9 (d) μs after 585 nm laser excitation. Time profiles of the Q_1 and D_0 signals were measured at positions indicated by the Q_1 and D_0 arrows, respectively. Fitted curves were calculated by a least-squares method.

distance and smaller number of bridging atoms between the SiPc and nitroxide nitrogen. This explanation is strongly supported by a previous study on the metal−nitroxide interaction, where the electron exchange interaction of the PROXYL derivative was found to be about 15 times larger than that of the TEMPO derivative.[10] Therefore, it is clarified experimentally that the lifetime of the excited multiplet state correlates well with the magnitude of the electron exchange interaction between the excited triplet SiPc and doublet NO radical.

Another finding is a difference between the −O− and −OCO− bridges. The lifetimes of R1a and R1c (−O− bridge) are about half of those of R1b and R1d (−OCO− bridge), respectively. These can also be explained by the concept that the electron exchange interaction via the −O− bridge is larger than that via the −OCO− bridge due to the shorter distance and smaller number of the bridging atoms.

TREPR Measurements. Steady-state EPR and TREPR spectra of R1a, R1b, and R1d at room temperature are shown in Figures 3, 4, and 5, respectively. For all complexes, a broad *A* signal ($g = 2.004 \pm 0.001$) is seen at 0.1 μs after laser excitation. Here, *A* and *E* denote absorption and emission of the microwaves, respectively. By comparison with the calculated *g* values,[16,17] the broad *A* signals are assigned to the Q_1 state, similar to R1c.[8a] The ESP behavior of the Q_1 state is divided into PROXYL (R1a and R1b) and TEMPO (R1c and R1d) groups, as follows. For R1a and R1b, the *A* polarization in the Q_1 state changes into *E* polarization. This kind of ESP inversion is similar to the C_{60}−NO and MP−nitpy systems.[6,7] On the other hand, for R1d, the *A* polarization in the Q_1 state decays without this kind of ESP inversion, in analogy with R1c.[8a] To discuss the results quantitatively, time profiles of the Q_1 signals were measured and are shown in Figures 3e, 4e, and 5e.[18] All time profiles of the Q_1 signals were analyzed with double-exponential functions (Table 2). For R1a and R1b, the ESP inversion from *A* to *E* is clearly shown, and the inversion time of the ESP and decay time of the *E* polarization are very short. Here, the decay times of the *E* polarization indicate the lifetime or the spin−lattice relaxation (SLR) time in the Q_1 state. For R1d, the decay profile of the *A* signal consists of two parts, fast and slow decays. Since the decay time ($=16 \pm 2$ μs) of the slow *A* signal is similar to that ($=15 \pm 0.9$ μs) of the transient absorption signal, the

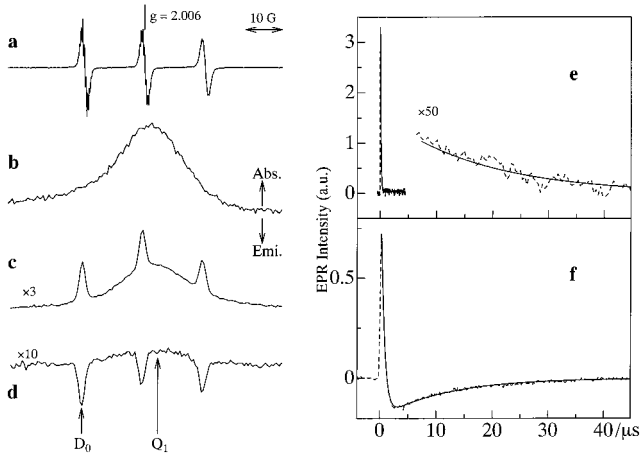

Figure 5. Steady-state EPR spectrum (a), TREPR spectra (b, c, d), and time profiles of the Q_1 and D_0 signals (e, f; broken lines) of R1d, together with fitted curves (e, f; solid lines). TREPR spectra were observed at 0.1 (b), 0.7 (c), and 2.5 (d) μs after 585 nm laser excitation. Time profiles of the Q_1 and D_0 signals were measured at positions indicated by the Q_1 and D_0 arrows, respectively. Fitted curves were calculated by a least-squares method.

TABLE 2: Inversion and Decay Times of the TREPR Signals

compd	signals	τ_1/μs	τ_2/μs
R1a	Q_1	≤ 0.1	0.47 ± 0.02
	D_0	0.54 ± 0.04	1.1 ± 0.1
R1b	Q_1	0.12 ± 0.03	0.69 ± 0.04
	D_0	0.77 ± 0.05	1.2 ± 0.1
R1c[a]	Q_1	≤ 0.1	5.1 ± 0.9
	D_0	0.71 ± 0.04	5.5 ± 0.6
R1d	Q_1	≤ 0.1	16 ± 2
	D_0	0.60 ± 0.03	13 ± 1

[a] From ref 8d.

fast and slow decay times can be reasonably assigned to the SLR time and lifetime of the Q_1 state, respectively.

For all complexes, three sharp *A* signals of the D_0 state are initially seen, which change into the *E* polarizations. Time profiles of the D_0 signals are shown in Figures 3f, 4f, and 5f, and were analyzed with double-exponential functions.[18] The inversion times of the ESP and decay times of the *E* polarization

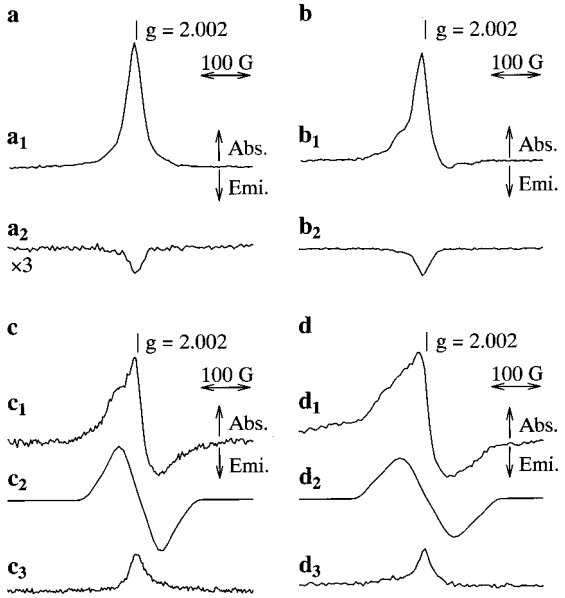

Figure 6. TREPR spectra of R1a (a), R1b (b), R1c (c), and R1d (d) at 20 K. TREPR spectra were observed at 0.6 (a_1, b_1, c_1, and d_1), 4.4 (b_2, c_3, and d_3), and 16.5 (a_2) μs after 585 nm laser excitation. Simulation spectra (c_2 and d_2) were calculated using parameters described in the text.[8a]

in the D_0 state are summarized in Table 2. Since the first *A* polarizations in the D_0 state are the same as those in the Q_1 state, they must originate from ESP transfer from the Q_1 state to the D_0 state.

On the other hand, the later *E* polarizations in the D_0 state are divided into two groups by reference to the Q_1 polarization. For R1d, the *E* polarization in the D_0 state is seen at 2.5 μs, in contrast to the *A* signal of the Q_1 state. In analogy with R1c, this ESP can be reasonably assigned to a radical−quartet pair mechanism (RQPM), where the excess α spin is produced by the intermolecular interaction between the Q_1 R1 and another R1.[8a,8d] It is found that the inversion time (=0.60 ± 0.03 μs) of the ESP and the decay time (=13 ± 1 μs) of the *E* polarization are almost identical to the SLR time (=0.55 ± 0.03 μs) of the D_0 state and decay time (=16 ± 2 μs) of the *A* signal of the Q_1 state.[19] This similarity strongly supports the RQPM assignment, since the rise and decay times of the RQPM have been evaluated as the SLR time of the D_0 state and lifetime of the Q_1 state, respectively.[8d,20]

For R1a and R1b, the later *E* polarization in the D_0 state is identical to that in the Q_1 state and appears to be explained by ESP transfer from the Q_1 state to the D_0 state. However, it is noteworthy that the decay times (R1a = 1.1 μs, R1b = 1.2 μs) of the *E* polarization in the D_0 state are close to the lifetimes (R1a = 0.86 μs, R1b = 1.4 μs) measured by transient absorption signals rather than the decay times (R1a = 0.47 μs, R1b = 0.69 μs) of the *E* polarization in the Q_1 state and SLR times (R1a = 0.56 ± 0.06 μs, R1b = 0.66 ± 0.03 μs) of the D_0 state.[19] Therefore, for R1a and R1b, we conclude that the *E* polarization in the D_0 state originates not only from the transfer of the Q_1 ESP but also from the RQPM and that the decay time of the *E* polarization in the D_0 state shows the Q_1 lifetime.[8d,20] In addition, the decay time of the *E* polarization in the Q_1 state is reasonably assigned to the SLR time of the Q_1 state, since it is shorter than that in the D_0 state.

To remove the intermolecular process, TREPR measurements were carried out at 20 K. TREPR spectra of R1a, R1b, and R1d are shown in Figure 6 together with those of R1c. The TREPR spectrum of R1c (Figure 6c) consists of two parts:[8a] One part is a central sharp D_0 signal at around $g = 2.00$. The other is an outer Q_1 signal with an *A*/*E* polarization. For R1d, the Q_1 signal was reproduced using $D = 0.170$ GHz, $E = 0.02$ GHz, and $P_{+3/2}:P_{+1/2}:P_{-1/2}:P_{-3/2} = 0:1:1:0$.[7] Since the *D* value (=0.170 GHz) obtained experimentally is almost identical to that (=0.14 GHz) calculated under a point charge approximation,[7,8,16] the outer *A*/*E* signals are clearly assigned to the Q_1 state. The *D* value (=0.170 GHz) of R1d is larger than that (=0.130 GHz) of R1c, reflecting a difference in the magnetic dipole−dipole interaction between the excited triplet SiPc and doublet NO.[7,8] It is found that the intensity of the *A*/*E* polarization in the Q_1 state compared with that of the *A* signal of the D_0 state decreases in the order R1d > R1c > R1b > R1a. Furthermore, the *A* polarization in the D_0 state changes into *E* polarization for R1a and R1b, while the *A* signal of the D_0 state decays without this ESP inversion for R1c and R1d.

Discussion

Lifetimes. All decay profiles of the transient absorption signals were analyzed using single-exponential functions. The lifetimes of SiPc-NO derivatives are much shorter than that of R0 (=500 μs), and originate from generation of the spin-allowed transition ($D_1 \rightarrow D_0$).[21,22] The lifetime decreases in the order R1d (=15 μs) > R1c (=7.6 μs) > R1b (=1.4 μs) > R1a (=0.86 μs) and is markedly dependent on the linking NO radicals. We will now try to analyze the excited-state lifetime quantitatively.

Since all decay profiles of the transient absorption signal are analyzed with a single-exponential function, the decay rate is given by $(2k_Q + k_D)/3$, where the k_Q and k_D denote the rate constants of the $Q_1 \rightarrow D_0$ and $D_1 \rightarrow D_0$ transitions, respectively.[8d,23,24] By reference to the $T_1 \rightarrow S_0$ transition, the decay rate of the $Q_1 \rightarrow D_0$ transition is evaluated as follows:[25]

$$k_{Qij} = (2\pi/3)|V_{ij}|^2\,\mathrm{Fc}(\Delta E) \tag{1a}$$

$$|V_{ij}|^2 = (e\tau/2)\sum_p |(\delta/\delta Q_p)\langle D_0,j|H_{SO}|Q_1,i\rangle|^2 \tag{1b}$$

$$i = \pm 1/2 \text{ or } \pm 3/2,\ j = \pm 1/2$$

Here, Fc is the Franck−Condon factor, which depends on the energy gap, ΔE. The electronic matrix element, V_{ij}, is approximated by the matrix element of the SOC operator (H_{SO}) with respect to the coordinate Q_p. Since the electronic interaction between the excited triplet SiPc and doublet NO is weak, the wave functions of the D_0 and Q_1 states are represented using wave functions of SiPc in the T_1 ($|\Psi_{Tk}\rangle$; $k = x, y, z$) and S_0($|\Psi_S\rangle$) states and NO radical in the D_0 state ($|\Psi_{R\pm}\rangle$) as follows:

$$|D_0, \pm 1/2'\rangle = |\Psi_S\Psi_{R\pm}\rangle \tag{2a}$$

$$|Q_1, \pm 3/2'\rangle = |\Psi_{T\pm}\Psi_{R\pm}\rangle \tag{2b}$$

$$|Q_1, \pm 1/2'\rangle = \{|\Psi_{T\pm}\Psi_{R\mp}\rangle + \sqrt{2}|\Psi_{Tz}\Psi_{R\pm}\rangle\}/\sqrt{3} \tag{2c}$$

$$|\Psi_{T\pm}\rangle = \mp 1/\sqrt{2}(|\Psi_{Tx}\rangle \pm i\,|\Psi_{Ty}\rangle) \tag{2d}$$

Since only the SOC between the Ψ_{Tk} and Ψ_S is significant, the matrix elements of the SOC are approximated by those represented by the singlet and triplet wave functions. Assuming that the Fc(ΔE) is unchanged by the NO substitution, the decay rate constant of the Q_1 state is expressed as follows:

$$k_Q = (1/4)\sum_i \sum_j k_{Qij}$$
$$= (1/4)(2\pi/3)(e\tau/2)Fc(\Delta E)\sum_i \sum_j \sum_p |(\delta/\delta Q_p)\langle D_0,j|H_{SO}|Q_1,i\rangle|^2$$
$$= (1/3)(2\pi/3)(e\tau/2)Fc(\Delta E)\sum_k \sum_p |(\delta/\delta Q_p)\langle \Psi_S|H_{SO}|\Psi_{Tk}\rangle|^2$$
$$= (1/3)\sum_k k_{Tk} = k_T \quad (3)$$

Here, the k_T and k_{Tk} denote the decay rates of the $T_1 \rightarrow S_0$ and $T_{1k} \rightarrow S_0$ transitions, respectively. Since the a_{1u} and e_g orbitals almost localize on SiPc and two axial oxygens, the k_Q values of all complexes were reasonably assumed to be identical and empirically evaluated as $2 \times 10^3\ s^{-1}$ ($=k_T$). Using this k_Q value, the k_D values were calculated as 3.5×10^6, 2.1×10^6, 3.9×10^5, and $2.0 \times 10^5\ s^{-1}$ for R1a, R1b, R1c, and R1d, respectively. The k_D values of R1a and R1b are about 10 times larger than those of R1c and R1d, respectively. Furthermore, the k_D values of R1a and R1c are about twice as large as those of R1b and R1d, respectively. Since the D_1-D_0 transition occurs accompanying an electron exchange process between the SiPc and NO moieties, $e_g \rightarrow r$ and $r \rightarrow a_{1u}$ (r denotes the SOMO of the NO radical),[26] these relationships can be reasonably interpreted by considering that the electron exchange interactions of the PROXYL and the −O− bridge are larger than those of the TEMPO and the −OCO− bridge, respectively.

In conclusion, it is shown experimentally that the decay rate of the D_1-D_0 transition is well-correlated with the magnitude of the electron exchange interaction between the excited triplet SiPc and doublet NO radical.

Q_1 ESPs. Two kinds of the Q_1 ESP behavior are observed at room temperature. For the PROXYL derivatives, the *A* polarization in the Q_1 state changes into the *E* polarization. On the other hand, for the TEMPO derivatives, the *A* polarization in the Q_1 state decays without ESP inversion. From here, the difference in the Q_1 ESP behavior will be discussed.

In the beginning, the Q_1 ESP behavior is considered for the D_1-Q_1 mixing and SOC cases. For D_1-Q_1 mixing, a contribution of the D_1 character to the Q_1 sublevels results in a spin-sublevel dependence on intersystem crossing (ISC). When $J < 0$, the D_1 character in the lower Q_1 sublevels is larger than that in the higher Q_1 sublevels, producing a situation in which the population and depopulation rates of the lower Q_1 sublevels are much faster than those of the higher Q_1 sublevels. When the depopulation time, $1/k_D$, competes with the SLR time of the excited state, the spin-selective ISC provides the ESP inversion. In the case of the SOC, the spin-selective ISC occurs, since the SOC with the doublet state depends on the Q_1 sublevels. This ESP can be also reversed,[27] when the $1/k_Q$ value is shorter than the SLR time, where k_Q indicates the depopulation rate promoted only by SOC. That is, the origin of the ESP inversion can be easily checked by comparing among the $1/k_D$, $1/k_Q$, and SLR time.

In our system, since the $1/k_Q$ value ($=500\ \mu s$) is much longer than the SLR time ($<1\ \mu s$), the ESP due to SOC decays without ESP inversion for all complexes. For the TEMPO derivatives, the $1/k_D$ values (R1c $= 2.6\ \mu s$, R1d $= 5.0\ \mu s$) are longer than the SLR times ($\leq 0.1\ \mu s$), indicating that the ESP inversion is not possible, even through D_1-Q_1 mixing. On the other hand, the ESP can be reversed for the PROXYL derivatives, since the $1/k_D$ values (R1a $= 0.29\ \mu s$, R1b $= 0.48\ \mu s$) are comparable to the SLR times (R1a $= 0.47\ \mu s$, R1b $= 0.69\ \mu s$). Therefore, it is found that the Q_1 ESP behavior at room-temperature originates from D_1-Q_1 mixing for the PROXYL derivatives, while it can be interpreted by both SOC and D_1-Q_1 mixing for the TEMPO derivatives.

Next, the TREPR results at 20 K are considered in order to clarify origins of the Q_1 ESP. For the PROXYL derivatives, the strong *A* polarization in the D_0 state changes into *E* polarization. In analogy with the TREPR results at room temperature, this ESP inversion of the D_0 signal is interpreted by D_1-Q_1 mixing. Since the *A/E* polarization in the Q_1 state, which originates from SOC, is very weak or does not exist, it is found that D_1-Q_1 mixing is preferable to SOC. In contrast, for the TEMPO derivatives, the Q_1 *A/E* polarization is clearly seen without ESP inversion of the D_0 signal, indicating that SOC is more efficient than D_1-Q_1 mixing. Therefore, the initial *A* polarization in the Q_1 state at room temperature can be reasonably assigned as originating from SOC for the TEMPO derivatives. As a result, we can conclude that the D_1-Q_1 mixing and SOC are preferable for the PROXYL and TEMPO derivatives, respectively, and that the Q_1 ESP due to the D_1-Q_1 mixing needs a relatively strong electron exchange interaction between the excited triplet SiPc and doublet NO, though the Q_1 ESP due to SOC is produced even by the weaker interaction.

Conclusions

We have studied derivatives of SiPc covalently linked to one NO radical and succeeded in clarifying the relationship between the Q_1 ESP, excited multiplet lifetime, and electron exchange interaction. It is shown experimentally that the rate of the D_1-D_0 transition correlates well with the electron exchange interaction and that the ESP of the radical−triplet pair changes from SOC type to D_1-Q_1 mixing type with increasing exchange interaction. These relationships are important for understanding the excited-state dynamics of the radical−triplet pair system.

Acknowledgment. This work was partially carried out in the Advanced Instrumental Laboratory for Graduate Research of the Department of Chemistry, Graduate School of Science, Tohoku University, and was supported by a Grant-in-Aid for Scientific Research (B) No. 11440192 and for Encouragement of Young Scientists No. 12740355 from the Ministry of Education, Science, Sports, and Culture, Japan.

References and Notes

(1) (a) Kuzmin, V. A.; Tatikolov, A. S.; Borisevich, Yu. E. *Chem. Phys. Lett.* **1978**, *53*, 52. (b) Kuzmin, V. A.; Tatikolov, A. S. *Chem. Phys. Lett.* **1978**, *53*, 606. (c) Watkins, A. R. *Chem. Phys. Lett.* **1980**, *70*, 262. (d) Schwerzel, R. E.; Caldwell, R. A. *J. Am. Chem. Soc.* **1973**, *95*, 1382. (e) Caldwell, R. A.; Schwerzel, R. E. *J. Am. Chem. Soc.* **1972**, *94*, 1035. (f) Chattopadhyay, S. K.; Das, P. K.; Hug, G. L. *J. Am. Chem. Soc.* **1983**, *105*, 6205. (g) Watkins, A. R. *Chem. Phys. Lett.* **1974**, *29*, 526. (h) Green, J. A., II; Singer, L. A.; Parks, J. H. *J. Chem. Phys.* **1973**, *58*, 2690. (i) Green, J. A., II; Singer, L. A. *J. Am. Chem. Soc.* **1974**, *96*, 2730.

(2) (a) Gouterman, M. In *The Porphyrins*; Dolphin, D., Ed.; Academic: New York, 1978; Vol. 3, pp 1−165. (b) Ferraudi, G. In *Phthalocyanines Properties and Applications*; Leznoff, C. C., Lever, A. B. P., Eds.; VCH Publishers: New York, 1989; Vol. I, pp 291−340.

(3) (a) Rosenthal, I.; Ben-Hur, E. In *Phthalocyanines Properties and Applications*; Leznoff, C. C., Lever, A. B. P., Eds.; VCH Publishers: New York, 1989; Vol. I, pp 393−425. (b) Rosenthal, I. In *Phthalocyanines Properties and Applications*; Leznoff, C. C., Lever, A. B. P., Eds.; VCH Publishers: New York, 1996; Vol. IV, pp 481−514, and many references therein.

(4) (a) Blättler, C.; Jent, F.; Paul, H. *Chem. Phys. Lett.* **1990**, *166*, 375. (b) Kawai, A.; Okutsu, T.; Obi, K. *J. Phys. Chem.* **1991**, *95*, 9130. (c) Kawai, A.; Obi, K. *J. Phys. Chem.* **1992**, *96*, 52. (d) Kawai, A.; Obi, K. *Res. Chem. Intermed.* **1993**, *19*, 865. (e) Turro, N. J.; Khudyakov, I. V.;

Bossmann, S. H.; Dwyer, D. W. *J. Phys. Chem.* **1993**, *97*, 1138. (f) Jockusch, S.; Dedola, G.; Lem, G.; Turro, N. J. *J. Phys. Chem. B* **1999**, *103*, 9126. (g) Corvaja, C.; Franco, L.; Pasimeni, L.; Toffoletti, A.; Montanari, L. *Chem. Phys. Lett*. **1993**, *210*, 355. (h) Corvaja, C.; Franco, L.; Toffoletti, A. *Appl. Magn. Reson*. **1994**, *7*, 257. (i) Corvaja, C.; Franco, L. Pasimeni, L.; Toffoletti, A. *J. Chem. Soc., Faraday Trans*. **1994**, *90*, 3267. (j) Hugerat, M.; van der Est, A.; Ojadi, E.; Biczok, L.; Linschitz, H.; Levanon, H.; Stehlik, D. *J. Phys. Chem*. **1996**, *100*, 495. (k) Regev, A.; Galili, T.; Levanon, H. *J. Phys. Chem*. **1996**, *100*, 18502.

(5) (a) Fujisawa, J.; Ishii, K.; Ohba, Y.; Iwaizumi, M.; Yamauchi, S. *J. Phys. Chem*. **1995**, *99*, 17082. (b) Fujisawa, J.; Ohba, Y.; Yamauchi, S. *J. Phys. Chem*. *A* **1997**, *101*, 434. (c) Jenks, W. S.; Turro, N. J. *Res. Chem. Intermed*. **1990**, *13*, 237.

(6) (a) Corvaja, C.; Maggini, M.; Prato, M.; Scorrano, G.; Venzin, M. *J. Am. Chem. Soc.* **1995**, *117*, 8857. (b) Corvaja, C.; Maggini, M.; Ruzzi, M.; Scorrano, G.; Toffoletti, A. *Appl. Magn. Reson.* **1997**, *12*, 477. (c) Mizuochi, N.; Ohba, Y.; Yamauchi, S. *J. Phys. Chem. A* **1997**, *101*, 5966. (d) Mizuochi, N.; Ohba, Y.; Yamauchi, S. *J. Phys. Chem. A* **1999**, *103*, 7749. (e) Mizuochi, N.; Ohba, Y.; Yamauchi, S. *J. Chem. Phys.* **1999**, *111*, 3479.

(7) (a) Ishii, K.; Fujisawa, J.; Ohba, Y.; Yamauchi, S. *J. Am. Chem. Soc.* **1996**, *118*, 13079. (b) Fujisawa, J.; Ishii, K.; Ohba, Y.; Yamauchi, S.; Fuhs, M.; Möbius, K. *J. Phys. Chem. A* **1997**, *101*, 5869. (c) Ishii, K.; Fujisawa, J.; Adachi, A.; Yamauchi, S.; Kobayashi, N. *J. Am. Chem. Soc.* **1998**, *120*, 3152. (d) Fujisawa, J.; Ishii, K.; Ohba, Y.; Yamauchi, S.; Fuhs, M.; Möbius, K. *J. Phys. Chem. A* **1999**, *103*, 213. (e) Ishii, K.; Ishizaki, T.; Kobayashi, N. *J. Phys. Chem. A* **1999**, *103*, 6060. (f) Ishii, K.; Kobayashi, N. *Coord. Chem. Rev.* **2000**, *198*, 231.

(8) (a) Ishii, K.; Hirose, Y.; Kobayashi, N. *J. Phys. Chem. A* **1999**, *103*, 1986. (b) Ishii, K.; Hirose, Y.; Kobayashi, N. *J. Am. Chem. Soc.* **1998**, *120*, 10551. (c) Ishii, K.; Hirose, Y.; Kobayashi, N. *J. Porphyrins Phthalocyanines* **1999**, *3*, 439. (d) Ishii, K.; Hirose, Y.; Kobayashi, N. *J. Am. Chem. Soc*. **2001**, *123*, 702.

(9) Recently, the excited multiplet studies have been reported for novel systems: (a) Asano-Someda, M.; van der Est, A.; Krüger, U.; Stehlik, D.; Kaizu, Y.; Levanon, H. *J. Phys. Chem. A* **1999**, *103*, 6704. (b) Teki, Y.; Miyamoto, S.; Iimura, K.; Nakatsuji, M.; Miura, Y. *J. Am. Chem. Soc.* **2000**, *122*, 984.

(10) Sawant, B. M.; Shroyer, A. L. W.; Eaton, G. R.; Eaton, S. S. *Inorg. Chem.* **1982**, *21*, 1093.

(11) Rozantzev, E. G.; Krinitzkaya, L. A. *Tetrahedron* **1965**, *21*, 491.

(12) Fukuju, T.; Yashiro, H.; Maeda, K.; Murai, H. *Chem. Phys. Lett.* **1999**, *304*, 173.

(13) Vincett, P. S.; Voigt, E. M.; Rieckoff, K. E. *J. Chem. Phys.* **1971**, *55*, 4131.

(14) Perkovic, M. W.; Ferraudi, G. *Inorg. Chim. Acta* **1997**, *254*, 1.

(15) Decay profiles were independent of the laser power, indicating that intramolecular quenching is more efficient than intermolecular quenching.

(16) (a) Bencini, A.; Gatteschi, D. *EPR of Exchange Coupled Systems*; Springer-Verlag: Berlin, 1990. (b) Kahn, O. *Molecular Magnetism*; Wiley−VCH: New York; 1993.

(17) g Values of the D_1 and Q_1 states were calculated as 1.998 and 2.002, respectively, by $g(D_1) = \{4g(T) - g(R)\}/3$ and $g(Q_1) = \{2g(T) + g(R)\}/3$,[16] where $g(T)$ (=2.000) and $g(R)$ (=2.006) denote g values of the excited triplet SiPc and doublet NO, respectively.

(18) Since time profiles of TREPR signals showed little dependence on the microwave power (=0.05−5 mW), the time profiles (microwave power = 5 mW) were quantitatively analyzed.

(19) The inversion recovery method was carried out using a $\pi-{}^{\pi}/_{2}$ pulse sequence.

(20) The time profile of the RQPM is expressed by $N = C_1 \exp(-k_M t) - C_2 \exp(-t/T_{1SLR}) + N_B$ (N_B = Boltzmann difference), where the two terms indicate the lifetime ($=1/k_M$) of the Q_1 state and SLR time ($=T_{1SLR}$) of the D_0 state.[8d]

(21) The energy transfer from the excited triplet SiPc to the doublet NO is negligible, since the energy (∼20 000 cm^{-1}) of NO in the lowest excited doublet state is much higher than that (∼9000 cm^{-1}) of the excited triplet SiPc.[13]

(22) (a) Weller, A. *Z. Phys. Chem. N. F*. **1982**, *133*, 93. (b) Osuka, A.; Nakajima, S.; Maruyama, K.; Mataga, N.; Asahi, T.; Yamazaki, I.; Nishimura, Y.; Ohna, T.; Nozaki, K. *J. Am. Chem. Soc.* **1993**, *115*, 4577. (c) Lever, A. B. P.; Minor, P. C. *Inorg. Chem.* **1981**, *20*, 4015. (d) Sudnik, M. V.; Romantsev, M. F. *J. Gen. Chem. USSR* **1972**, *42*, 735. (e) Tsunaga, M.; Iwakura, C.; Tamura, H. *Electrochim. Acta* **1973**, *18*, 241. (f) Tsunaga, M.; Iwakura, C.; Yoneyama, H.; Tamura, H. *Electrochim. Acta* **1973**, *18*, 615. (g) For R1c, charge transfer (CT) energies were estimated by $E(CT) = E_{ox} - E_{red} + (e^2/2)(1/r_D + 1/r_A)(1/4\pi\epsilon_0\epsilon - 1/4\pi\epsilon_0\epsilon_r) - e^2/4\pi\epsilon_0\epsilon R_{DA}$, where E_{ox} and E_{red} are oxidation potentials of the donor and reduction potential of the acceptor, respectively, measured in DMF; r_D and r_A are effective radii of the donor cation and acceptor anion; and ϵ_r and ϵ are the dielectric constants of DMF (=36.71) and toluene (=2.38), respectively.[22a,b] The radii of SiPc and TEMPO were taken to be 7.6 and 2.4 Å, respectively, and the separation (R_{DA}) between charges to be 5.75 Å. The E_{red} potentials of SiPc and TEMPO in DMF are −0.54 and −1.28 V (vs SCE), respectively.[22c,d] The E_{ox} potential of SiPc in DMF was calculated as 1.01 V (vs SCE) by $E_{ox} = 1170 - 11.7(r/ze)$ mV, where ze and r denote the charge (=+4) and radius (=54 pm) of silicon, respectively.[22c] The E_{ox} potential of TEMPO measured in acetonitrile (=0.62 V vs SCE) was employed for the CT calculations,[22e,f] since the dielectric constant of DMF (=36.71) is close to that of acetonitrile (=37.5). Using these values, the CT energies of $SiPc^+-TEMPO^-$ and $SiPc^--TEMPO^+$ in toluene were evaluated as 2.2×10^4 and 1.3×10^4 cm^{-1}, respectively. Since both CT energies are higher than the energy (∼9000 cm^{-1}) of the excited triplet SiPc, the CT can be ruled out.

(23) The typical Q_1 TREPR spectra are seen at 20 K for the TEMPO derivatives, indicating that the D_1-Q_1 splitting is ≥0.1 cm^{-1}. Therefore, we reasonably assumed that the D_1-Q_1 mixing is negligible in our transient absorption measurements, where the Zeeman splitting is absent. Ishii, K.; Ishizaki, T.; Kobayashi, N. Submitted.

(24) Asano, M.; Kaizu, Y.; Kobayashi, H. *J. Chem. Phys.* **1988**, *89*, 6567.

(25) van Dorp, W. G.; Schoemaker, W. H.; Soma, M.; van der Waals, J. H. *Mol. Phys.* **1975**, *30*, 1701.

(26) The D_n-D_1 interaction also consists of the electron exchange interactions between the r and a_{1u} or e_g orbitals. Ake, R. L.; Gouterman, M. *Theor. Chim. Acta* **1969**, *15*, 20.

(27) Yamauchi, S.; Hirota, N.; Higuchi, J. *J. Phys. Chem.* **1988**, *92*, 2129.